Rapid discrimination of crystal handedness by XNCD mapping

Miguel Cortijo, Ángela Valentín-Pérez, Andrei Rogalev, Fabrice Wilhelm, Philippe Sainctavit, Patrick Rosa, Elizabeth Anne Hillard

Rapid discrimination of crystal handedness using XNCD mapping

Dr. Miguel Cortijo[a, b] , Dr. Ángela Valentín-Pérez [a, b] , Dr. Andrei Rogalev[c] , Dr. Fabrice Wilhelm[c] , Dr. Philippe Sainctavit[d] , Dr. Patrick Rosa [a, b] , Dr. Elizabeth A. Hillard [a, b]

[a]*CNRS, ICMCB, UMR 5026, 33600 Pessac, France / Université de Bordeaux, ICMCB, UMR 5026, 33600 Pessac, France*
[b]*CNRS, ICMCB, UMR 5031, 33600 Pessac, France / Université de Bordeaux, CRPP, UMR 5031, 33600 Pessac, France*
[c]*European Synchrotron Radiation Facility (ESRF), 38043 Grenoble, France*
[d]*IMPMC, CNRS, Sorbonne Université, Muséum National d'Histoire Naturelle, UMR7590, 4 place Jussieu, 75252 Paris Cedex 05, France*

Abstract : An original method for determining the handedness of individual non-centrosymmetric crystals in a mixture using a tightly-focused, circularly polarized X-ray beam is presented. The X-ray natural circular dichroism (XNCD) spectra recorded at the metal K-edge on selected crystals of [Δ-M(en)$_3$](NO$_3$)$_2$ and [Λ-M(en)$_3$](NO$_3$)$_2$ (M=Co^{II}, Ni^{II}) show extrema at the metal pre-edge (7712 eV for Co, 8335 eV for Ni). A mapping of a collection of some 220 crystals was performed at the respective energies by using left and right circular polarizations. The difference in absorption for the two polarizations, being either negative or positive, directly yielded the handedness of the crystal volume probed by the beam. By using this technique, it was found that the addition of l-ascorbic acid during the synthesis of [Co(en)$_3$](NO$_3$)$_2$ resulted in an enantiomeric enrichment of the Λ-isomer of 67±13 %, whereas the Ni analogue was similarly, but conversely, enriched in the Δ-isomer (65±22 %).

Keywords : *Chirality ; Conglomerate crystallization ; Coordination chemistry ; X-ray absorption ; X-ray optical activity*

Supporting information : https://doi.org/10.1002/chem.202001783

Due to the thermodynamic equivalence of enantiomeric pairs, as well as the entropic stabilization of such mixtures, the laboratory synthesis of chiral species in solution results in racemic mixtures in the absence of a chiral auxiliary. Such racemates most often crystallize as centrosymmetric crystals comprising both enantiomers, while the formation of conglomerates, where the two antipodes crystallize in separate crystals, is estimated to occur in less than 10 % of racemic mixtures.[1] While crystals of only one or the other enantiomer can be effortlessly obtained by this process, such a spontaneous resolution can only truly be considered accomplished after the identification and triage of the two forms of crystals. In the famous experiment of Louis Pasteur, a conglomerate of sodium ammonium tartrate yielded hemihedral crystals, the separation of which could then be manually achieved by visual inspection of the crystal faces.[2] It is noteworthy that the reproduction of this experiment has only been accomplished with difficulty,[3] mainly due to irregular crystal facets, and that even in the ubiquitous mineral quartz, the occurrence of well-defined enantiomorphic faces occurs only rarely.[4]

Knowing the handedness of individual crystals in a mixture is of interest not only for selecting crystals for analysis, but also for the study of solid-state deracemization processes, which can have industrial applications.[5] Not long after Pasteur's experiment, enantioselective crystallization was accomplished by seeding with a homochiral crystal,[6] and when the compounds in solution are achiral or subject to fast racemization, this technique can yield enantiomeric excesses approaching 100 %.[7] Asymmetric enrichment can also occur during the crystallization of optically inactive solutions in the absence of a chiral auxiliary.[8] While this stochastic deracemization technique has been shown to occur in organic systems,[9] much of the work in this area has been performed on crystals where the dissymmetry arises from a helicoidal arrangement of achiral species, mainly NaClO$_3$.[10] In one of the first such demonstrations, over 10 000 individual NaClO$_3$ crystals were examined for the publication.[11] Because such processes rely on (secondary) nucleation phenomena, the handedness of the individual crystals is the metric of interest, rather than the molecular enantiomeric excess.

Analysis of chirality in the solid state is particularly challenging,[12] as linear dichroism and birefringence can be orders of magnitude more intense than the circular dichroism signal.[13] The interest of NaClO$_3$ in such studies is due to the advantages of crystallizing in a cubic crystal system, giving transparent mm-dimension crystals, and thus allowing chirality determination with a polarized optical microscope. Meanwhile, for small, anisotropic and/or colored crystals, X-ray crystallography is the method of choice, requiring a substantial time investment for data collection and treatment.

Here we present an X-ray natural circular dichroism (XNCD) mapping technique able to image with micrometer resolution the handedness of individual crystals. Like the more familiar electronic natural circular dichroism, the XNCD

spectrum is expressed as the difference of absorption spectra of right- and left- circularly polarized electromagnetic radiation, and can only be observed in non-centrosymmetric media. Unlike ECD, however, XNCD is only observable in ordered media, and more specifically in crystals belonging to one of 13 non-centrosymmetric crystal classes.[14] A major advantage in using XNCD is that the refraction index in the X-ray range is very close to unity, rendering linear and circular birefringence contributions much weaker. Moreover, XNCD measurements can be performed on optically dense crystals as well as on transparent ones.

For this demonstration, we chose to investigate crystals of the coordination compounds $[Co(en)_3](NO_3)_2$[15] and $[Ni(en)_3](NO_3)_2$,[16] which crystallize as conglomerates in the space group $P6_322$ at room temperature, providing uniaxial crystals adopting a rectangular block habit. During the synthesis of $[Co(en)_3](NO_3)_2$, l-ascorbic acid (AA), a naturally-occurring chiral compound, was added to discourage aerial oxidation of Co^{II}. Selective crystallization using a non-co-crystallizing dissymmetric additive is well known, involving a preferential interaction with the additive and one of the enantiomers, either in solid state or in solution.[5, 17]

Crystals of $[Co(en)_3](NO_3)_2$ and $[Ni(en)_3](NO_3)_2$, selected using single crystal X-ray diffraction, each show a distinct and strong XNCD signal at their respective K absorption edges. As shown in Figure 1, the spectra of the Δ and Λ enantiomers display the expected mutual mirror-image symmetry, particularly in the pre-edge features. The dichroism peaks of equal and opposite intensity at 7712.4 eV for Co and 8335.3 eV for Ni, thus provide a direct probe to determine the handedness of the crystal volume irradiated by the synchrotron X-ray beam spot.

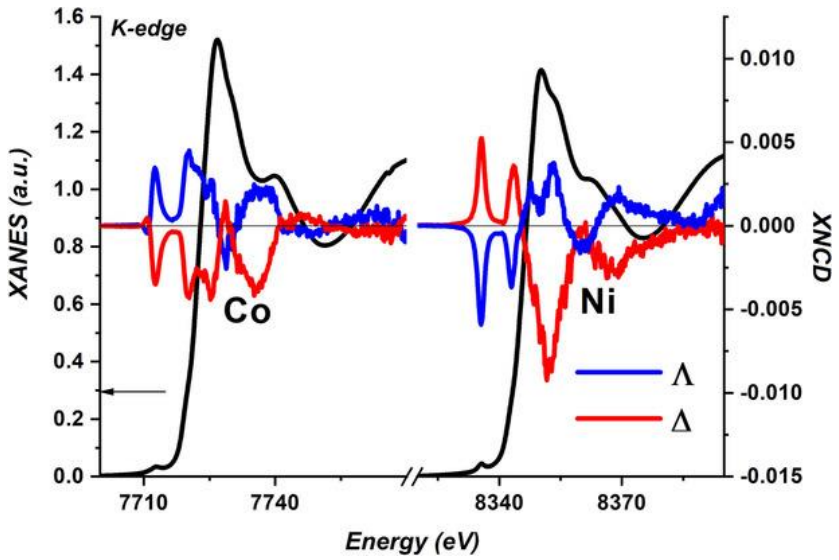

Figure 1 : XNCD (blue and red lines) and X-ray absorption near edge spectra (XANES, black lines) spectra for $[Co(en)_3](NO_3)_2$ and $[Ni(en)_3](NO_3)_2$.

From a single crystallization batch, 128 crystals of $[Co(en)_3](NO_3)_2$ were mounted on a sample plate using double-sided tape (Figure S1). Similarly, assemblies of 46 crystals from a batch of $[Ni(en)_3](NO_3)_2$ crystallized in the presence of AA and 46 crystals crystallized in the absence of AA were likewise mounted (Figure S1). The isomorphous crystals grow as rectangular blocks, such that the *c* crystal axis is oriented parallel to the long crystal dimension. As the crystallographic *a* and *b* axes are equal, the crystals could be easily mounted in the orthoaxial orientation by placing them so that the long crystal edge was parallel to the sample plate (and thus perpendicular to the beam). The X-ray fluorescence signal, proportional to the X-ray absorption, was measured at the pre-edge energy maximum, using a beam spot size restricted to 150(H)×50(V) μm^2, and alternating the circular polarization between right and left. The beam spot was then moved over the sample holder, yielding a mapping of the handedness of the individual crystals (Figure 2).

Averaging the two polarizations yielded the isotropic X-ray absorption signal, which was used to delineate the crystal contours as seen by the beam (Figure S2). Figure S3 shows the agreement between those contours with high-resolution optical images and Figure S4 reports a numbering Scheme for the three crystal assemblies contoured effectively by X-ray absorption, that is, only 127 crystals for $[Co(en)_3](NO_3)_2$, but the full 46+46 cohort for $[Ni(en)_3](NO_3)_2$. Figure 2 reports the raw dichroic signal in a red (Δ) to blue (Λ) scale, superimposed with the crystal contours (black lines). In the Figure, one observes rings around the edges of the crystals representing lower XNCD intensity. This is considered to be due to the beam being only partially on the crystal in these regions, thus resulting in a less intense unnormalized

absorption signal, and consequently a lower XNCD, and should not be considered representative of lower enantiopurity in these regions.

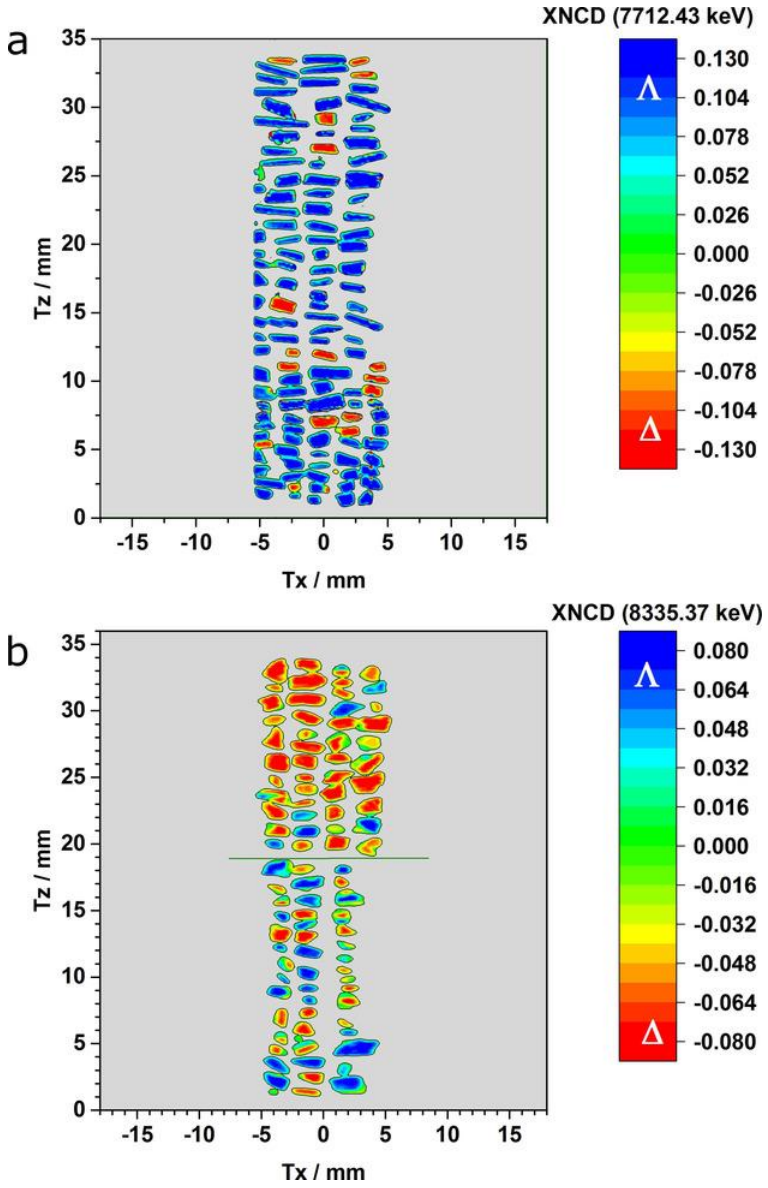

Figure 2 : NCD mapping of a) $[Co(en)_3](NO_3)_2$ and b) $[Ni(en)_3](NO_3)_2$. For $[Ni(en)_3](NO_3)_2$, the batch crystallized with AA is above the dark green line. Crystal contours as obtained from the X-ray absorption are reported as black lines.

It can readily be seen in Figure 2 that most crystals appear to consist of monodomains. We classified all crystals as either twinned, or predominantly or fully Δ or Λ (Table S1) In the case of $[Co(en)_3](NO_3)_2$, 9 crystals were considered as undetermined since less than half the crystal was actually measured. In a first approach we will ignore the twinned crystals (1 for $[Co(en)_3](NO_3)_2$ and 5 and 9 for $[Ni(en)_3](NO_3)_2$) and consider for a given crystal only the predominant handedness, which yields populations of 117 crystals for $[Co(en)_3](NO_3)_2$ and 41 and 37 crystals for $[Ni(en)_3](NO_3)_2$.

Of the 117 measured crystals in the $[Co(en)_3](NO_3)_2$ assembly, 18 were found to be in the delta configuration, while the remaining 99 crystals were in the lambda configuration. Crystalline enantiomeric enrichment, but in the opposite direction, was found for the $[Ni(en)_3](NO_3)_2$ group where AA was added: over 41 crystals, six crystals were lambda in configuration, and 35 crystals had the delta configuration. Crucially, for the $[Ni(en)_3](NO_3)_2$ set of 37 crystals without AA, no significant enantiomeric enrichment was revealed: 20 crystals were lambda, and 17 were delta.

The enantiomeric excess (*ee*) of the individual crystals was calculated from the mapping data by determining the probability *p* of obtaining a crystal of a given handedness and its corresponding confidence interval, using the Agresti–Coull interval.[18] In the cobalt case, *p* was found in the interval [0.769;0.901] at the 95 % confidence level, which is equivalent to an *ee* of lambda crystals between 54 % and 80 %, while the Ni batch crystallized with AA gave a crystal

ee between 43 % and 86 % for the delta isomer. For the Ni batch crystallized without AA, the crystal *ee* is found between −23 % and 38 %. This latter batch is thus seen as having a crystal *ee* not statistically different from zero, that is, not distinguishable from a perfect conglomerate. On the other hand, the presence of AA does induce a statistically significant optical enrichment of the two complexes, with non-zero crystal *ee* values, but in opposite directions. While bias in conglomerate crystallization has been observed due to chiral contaminants,[17] this appears to be an unusual case where two isomorphous compounds, crystallized under the same conditions, show an opposite enantiomeric enrichment.

An important aspect of this mapping technique is its spatial resolution. When considering the crystals categorized as "twinned", it is noteworthy that they are twice as abundant for $[Ni(en)_3](NO_3)_2$ when crystallized without AA, *viz*. there are nine examples of twinned crystals in the batch without AA and five twinned crystals when AA was used. Two examples of truly racemic crystals were found, for $[Ni(en)_3](NO_3)_2$ crystallized with or without AA (Figure S5), appearing as neither Δ nor Λ, at least down to the spatial resolution available on the beamline at the time of these experiments. Racemic crystals are quite unexpected for this system thought to be a conglomerate, and would point either towards crystals of a different centrosymmetric phase or a true racemic twin, which is not a frequent occurrence. The other crystals classified as twinned appear as two or three coexisting domains of a given handedness, with quite large separations respective to the beam spot size (Figure S6). Otherwise the mapping of the crystals shows a quite interesting difference between $[Co(en)_3](NO_3)_2$ and $[Ni(en)_3](NO_3)_2$: for $[Co(en)_3](NO_3)_2$, the domains are very pronounced, with narrow delimiting regions (see Figure 2). For $[Ni(en)_3](NO_3)_2$, the domain borders seem to be softer, with large regions being almost racemic (see green zones in Figure 2). These observations suggest a difference in the crystallization process for $[Co(en)_3](NO_3)_2$ and $[Ni(en)_3](NO_3)_2$, which may account for the opposed chiral induction shown by the AA. In order to unambiguously confirm the role of the AA on the enantiomeric enrichment of these complexes, studies on the effect of its concentration, as well as the effect of its optical isomer, d-ascorbic acid, are planned.

In conclusion, these results show that XNCD mapping provides a general method for determining the handedness of individual non-centrosymmetric crystals in an assembly. This technique is particularly pertinent when the handedness of individual crystals, rather than molecular *ee*, is sought, such as in the study of solid-state deracemization processes,[9, 10] like Viedma ripening or temperature cycling. It also of interest for chiral systems that cannot be studied by standard solution-based methods, such as HPLC, due to rapid racemization, as is the case herein and for many first-row transition metal complexes, or when chirality is only induced by crystal packing of achiral molecules. Moreover, it allows the imaging of anisotropic crystals of submillimeter dimensions, and is applicable to even highly colored crystals, in which optical microscopy cannot clearly differentiate the difference in light transmittance. Finally, we have shown the use of this technique in the imaging of chiral domains in a single crystal. Following the extremely brilliant source (EBS) upgrade, the ID12 beamline of the ESRF will offer enhanced capabilities for XNCD mapping using a much smaller symmetric beam of about 2 µm diameter over the energy range from 2 to 15 keV. This upgrade would allow access to detailed domain maps within a twinned crystal, which may eventually shed light on dissymmetric nucleation processes.

Acknowledgements : This work was supported by the CNRS, the University of Bordeaux, the Conseil Régional de la Nouvelle Aquitaine, the European Union's Horizon 2020 research and innovation program under the Marie Sklodowska-Curie grant agreement No 706556 CHIMMM (Postdoctoral fellowship for MC), the French Ministry of Higher Education, Research and Innovation (PhD bursary for AVP), and the European Synchrotron Radiation Facility (beamtime CH-5531). The authors thank R. Clérac for useful discussions.

Conflict of interest : The authors declare no conflict of interest.

1- L. L. Pérez-García, D. B. Amabilino, *Chem. Soc. Rev.* 2002, 31, 342.
2- L. Pasteur, *Ann. Chim. Phys.* 1848, 24, 442.
3- Y. Tobe, *Mendeleev Commun.* 2003, 13, 93.
4- A. M. Glazer, *J. Appl. Crystallogr.* 2018, 51, 915.
5- 5a C. Rougeot, J. E. Hein, *Org. Process Res. Dev.* 2015, 19, 1809; 5b R. M. Secor, *Chem. Rev.* 1963, 63, 297.
6- D. Gernez, *Compt. Rend. Acad. Sci.* 1866, 63, 843.
7- 7a G. Levilain, G. Coquerel, *CrystEngComm* 2010, 12, 1983; 7b A. Collet, M.-J. Brienne, J. Jacques, *Chem. Rev.* 1980, 80, 215.
8- 8a R. E. Pincock, K. R. Wilson, *J. Chem. Educ.* 1973, 50, 455; 8b S.-T. Wu, Y.-R. Wu, Q.-Q. Kang, H. Zhang, L.-S. Long, Z. Zheng, R.-B. Huang, L.-S. Zheng, *Angew. Chem. Int. Ed.* 2007, 46, 8475; / *Angew. Chem.* 2007, 119, 8627; 8c W. L. Noorduin, H. Meekes, A. A. C. Bode, W. J. P. van Enckevort, B. Kaptein, R. M. Kellogg, E. Vlieg, *Cryst. Growth Des.* 2008, 8, 1675.
9- 9a E. Havinga, *Biochem. Biophys. Acta* 1954, 13, 171; 9b A. C. D. Newman, H. M. Powell, *J. Chem. Soc.* 1952, 3747; 9c R. E. Pincock, K. R. Wilson, *J. Am. Chem. Soc.* 1971, 93, 1291; 9d R. E. Pincock, R. R. Perkins, A. S. Ma, K. R. Wilson, *Science* 1971, 174, 1018; 9e F. Cameli, J. H. Ter Horst, R. R. E. Steendam, C. Xiouras, G. D. Stefanidis, *Chem. Eur. J.* 2020, 26, 1344; 9f C. Xiouras, E. Van Cleemput, A. Kumpen, J. H. Ter Horst, T. Van Gerven, G. D. Stefanidis, *Cryst. Growth Des.* 2017, 17, 882; 9g K. Suwannasang, A. E. Flood, C. Rougeot, G. Coquerel, *Cryst. Growth Des.* 2013, 13, 3498; 9h W. W. Li, L. Spix, S. C. A. De Reus, H. Meekes, H. J. M. Kramer, E. Vlieg, J. H. Ter Horst, *Cryst. Growth Des.* 2016, 16, 5563; 9i F. Breveglieri, G. M. Maggioni, M. Mazzotti, *Cryst. Growth Des.* 2018, 18, 1873; 9j G. M. Maggioni, M. P. Fernández-Ronco, M. van de Meijden, R. M. Kellogg, M. Mazzotti, *CrystEngComm* 2018, 20, 3828; 9k K. Suwannasang, A. E. Flood, C. Rougeot, G. Coquerel, *Org. Process Res. Dev.* 2017, 21, 623; 9l W. L. Noorduin, W. J. P. van Enckevort, H.

Meekes, B. Kaptein, R. M. Kellogg, J. C. Tully, J. M. McBride, E. Vlieg, *Angew. Chem. Int. Ed.* 2010, 49, 8435; / *Angew. Chem.* 2010, 122, 8613.
10- 10a W. S. Kipping, W. J. Pope, *J. Chem. Soc. Trans.* 1898, 73, 606; 10b C. Viedma, *Phys. Rev. Lett.* 2005, 94, 3; 10c C. Viedma, B. J. V. Verkuijl, J. E. Ortiz, T. De Torres, R. M. Kellogg, D. G. Blackmond, *Chem. Eur. J.* 2010, 16, 4932; 10d L.-C. Sögütoglu, R. R. E. Steendam, H. Meekes, E. Vlieg, F. P. J. T. Rutjes, *Chem. Soc. Rev.* 2015, 44, 6723; 10e C. Xiouras, J. H. Ter Horst, T. Van Gerven, G. D. Stefanidis, *Cryst. Growth Des.* 2017, 17, 4965; 10f C. Viedma, P. Cintas, *Chem. Commun.* 2011, 47, 12786.
11- D. K. Kondepudi, R. J. Kaufman, N. Singh, *Science* 1990, 250, 975.
12- W. Kaminsky, K. Claborn, B. Kahr, *Chem. Soc. Rev.* 2004, 33, 514.
13- R. Kuroda, T. Harada, Y. Shindo, *Rev. Sci. Instrum.* 2001, 72, 3802.
14- J. Goulon, A. Rogalev, F. Wilhelm, C. Goulon-Ginet, P. Carra, I. Marri, C. Brouder, *J. Exp. Theor. Phys.* 2003, 97, 402.
15- M. Cortijo, Á. Valentín-Pérez, M. Rouzières, R. Clérac, P. Rosa, E. A. Hillard, *Crystals* 2020, 10, 472.
16- L. J. Farrugia, P. Macchi, A. Sironi, *J. Appl. Crystallogr.* 2003, 36, 141.
17- 17a J. Jacques, A. Collet, S. H. Wilen in Enantiomers, Racemates and Resolutions, Krieger Publishing Company, Malabar, 1994, pp. 245–250; 17b I. Weissbuch, L. Addadi, M. Lahav, L. Leiserowitz, *Science* 1991, 253, 637; 17c A. H. J. Engwerda, P. van Schayik, H. Jagtenberg, H. Meekes, F. P. J. T. Rutjes, E. Vlieg, *Chem. Eur. J.* 2018, 24, 2863; 17d J.-M. Cruz, K. Hernández-Lechuga, I. Domínguez-Valle, A. Fuentes-Beltrán, J. U. Sánchez-Morales, J. L. Ocampo-Espindola, C. Polanco, J.-C. Micheau, T. Buhse, *Chirality* 2020, 32, 120.
18- A. Agresti, B. A. Coull, *Am. Stat.* 1998, 52, 119.